

Tribological Properties And Heat Treatment On Aluminium A356 Bolstered With Bottom Ash Metallic Matrix Composites

^[1]H S Sridhar ^[2]Batluri Tilak Chandra ^[3]Sunil Kumar M ^[4]Jagannatha N

^[1]Department of Mechanical Engineering, Sri Siddhartha Academy of Higher Education, Tumkur, Karnataka, India

^[2]Professor, Mechanical Engineering, SSIT, Tumkur, Karnataka, India

^[3]Research scholar VTURRC Belgaum, Karnataka, India

^[4]Professor and Head, Mechanical Engineering, SJMIT, Chitradurga, Karnataka, India

Email: ^[1]sridharskit@gmail.com

Abstract: The key goal of this study is to investigate the impact of thermal treatment on the tribological attributes of Aluminium Metallic Matrix Composite (AMMCs). The metal structure of A356 is reinforced by bottom ash particles. The practise of stir casting is what leads to the development of the composite. Bottom ash particulates are reinforced at different weight percentage ranges from 0wt% - 8wt% in phases about 2wt%. Experiments were done with a pin-on-disk dry-slide wear assessment system to examine the wear behaviour. Various applied weights, sliding velocity values, and coefficients of resistance were tested while retaining the sliding distances and duration constant. The composites subjected to heat treatment exhibited improved resistance to wear in contrast to the composites that were not heat treated. Micrographic analysis is conducted by using patterns created by X-ray diffraction and pictures produced by electron microscopes (SEM). It was determined that there was a consistent distribution of bottom ash particulate matter in the A356 substrate alloy of composites, which was one of the findings from XRD that supported the presence of bottom ash particles.

1. Introduction

Aluminium alloy is playing an increasingly important part in modern industry, helping businesses achieve better results. As a result of their exceptional resistance to both wear and corrosion as well as their outstanding toughness, strength, and hardness, aluminium metal matrix composites find widespread use in many different industries, including as the aviation, automotive, and aerospace industries, defence industries, among others [1-3]. The incorporation of bottom ash, which consists of ceramic particles that are hard of iron ore, into the framework of aluminium demonstrates an improvement in the material's potential for use in regions subject to wear and tear [4]. The most prevalent method for the creation of composites made of metal matrix was called stir casting. Once the composite was created, it was put through a heat treatment, which had an influence in terms of mechanical, tribological, and microstructural characteristics [4, 5, 6]. According to another study's findings, Shankar subramanian et al., [7] A comprehensive analysis of the erosion performance of an aluminium alloy composite containing multiple reinforcements was documented. Results reveals composites supplemented with sugarcane bagasse ash along with particles of silicon carbide demonstrates greater wear resistance over as-cast composites. Wear resistance was shown to be higher in composite samples than in as-cast specimens when the casted Al6061 alloys was reinforced with flyash, copper, and graphite powder, as examined by S. Balakumar et al. [8]. Wear attributes of an aluminium (Al) 6061 mix with reinforcements of flyash, magnesium, and graphite at varying weight percentages are studied by Viney Kumar et al. [9], and the results demonstrate improved wear qualities of specimens made of materials. H S Sridhar et al., [27] Result shows The wear resistance of A356-bottom ashes composite rises with matrix alloy reinforcement percentage. The findings also demonstrate that composites containing 10 wt% bottom ash particles have strong abrasive wear resistance and weight loss as applied load rises. The highest and smallest weight decrease for all composites were 10 N and The behaviour of cinders amalgam composites in comparison to Al 7075 enriched burgundy under wear

conditions is studied by N. S. Mishra et al., [10]. The findings reveal that, in comparison to cinders armoured Al7075 amalgam composite, burgundy armoured Al7075 composite signify less evident wear tempo. Tribological characteristics of A356.2 alloy after being combined with the ash from rice husks at varying weight percentages as a reinforcing agent were published by D shiv prasad et al.[11], showing that the resulting composites had a greater susceptibility to wear than the unreinforced alloy. It has been shown that the temperature transition for aluminium-alloys with nanoparticles at different pressures and temperatures relies heavily on the nominal pressure. The only advantage that may be gained from the reinforcement is an increase in the transition temperature at higher levels. The wear rate is affected outermost layer of wear, which may take on a variety of shapes and have varying thicknesses. Within the moderate degradation regime, compound wear rates are even greater compared to that of the reinforced alloy. The tribological compliance of commercially available aluminium MMCs using graphite as a solid lubricate was investigated by Prasad S. V. and colleagues [13]. According to the findings, films burnished on surfaces of Al-Cu metals made possible to handle much higher pressures. compared to those burnished on surfaces made of Al-Si alloys. The tribological characteristics of an aluminium metal surface were investigated by Ahmer SM, et al.,[14] with a load of 196.2 N at a temperature of 300K. The first set of tests pits an aluminium pin against a steel disc coated with Helix oil, while the second pits an aluminium pin against a combination of 10% polytron, with the remaining 90% being Helix oil. Results demonstrate that aluminium surface wear only 20 m in the APS arrangement. APS wears down far more slowly than aluminium, by a factor of 0.33. Siva Prasad A Rama Krishna, et al.,[28] Mechanical, Tribological properties, SEM analysis were examined. According to the findings, composites have a greater level of hardness and resilience to wear in comparison to unreinforced aluminium alloy. In their study, Rohatgi P K, et al. (15) examined the incorporation of non-metallic substances into metallic substances or alloys as extra protection in order to create novel materials that exhibit enhanced tribological performance. The researchers investigated the influence of various parameters, including material settings, mechanical factors, and physical properties, on the performance of these metal matrix composites (MMCs). The findings indicate that the nano-composites exhibited superior frictional characteristics in comparison to the micro-composites. According to previous research, little research was previously done on A356-Bottom Ashes particle composites. In addition, the influence of reinforcing, applied stresses, moving velocities, and the corresponding coefficient of friction on A356 with Bottom Ash Particle MMCs is investigated.

2. Materials and Methods

2.1 Material Selection

The current work is on the utilisation of A356 compounds in slab form as a composite material. This is largely due to the wide applications the material has in the aerospace and automotive sectors.

Table 1: Chemical Constituents Of Alloy Of A356

Composition	Percentage
Si	7.25
Mg	0.45
Fe	0.086
Cu	0.010
Mn	0.018
Ni	0.025
Zn	0.005
Others	0.028
Al	92.12

For this purpose, we use Bottom Ash particles between 50 and 100 m in size. Tables 1 and 2 show the chemical compositions of the reinforcements and matrix alloys. Tables 3 and 4 display these materials' additional attributes.

Table 2: Chemical Constituents of Bottom Ash by Wt% of Construction

Constituents	Percentage
SiO ₂	65.50
CaO	2.80
Al ₂ O ₃	16.21
ZnO	0.020
MgO	0.75
Fe ₂ O ₃	4.90
TiO ₂	1.20
MnO	0.12
P ₂ O ₅	0.080
CuO	0.040
Loss of Ignition	2.58

Table 3: Attributes of A356 Alloy

Attributes	Values	Units
Colour	Silver	---
Tensile strength ultimate	234	Mpa or N/mm ²
Compressive strength	650	Mpa
Density	2.67	gm/cc
Hardness (Brinell)	70-105	---
Melting Point	557-613	°C
Tensile strength yield	165	Mpa or N/mm ²
Poisson's Ratio	0.33	Nu
Elastic Modulus	70-80	Gpa

Table 4: Attributes of Bottom Ash particles

Attributes	Values	Units
Particle Size	50-100	Mm
Density	2.6	gm/cc
Colour	Black	---
Hardness (Rockwell)	90	Kg/mm ²

2.2. Composite Preparation

The stir casting procedure, which is detailed in more detail below, is used in the production of the composite with metal matrix made of A356 alloys that are strengthened with Bottom Ash particles. Figure 1 shows A356 alloys being melted in a 6 kilowatt electric resistance furnace at a temperature of 752 degrees Celsius while maintaining a stirring speed of 560 revolutions per minute. Before being put into an oven that was preheated to 7500 degrees Celsius and contained a hot, molten substance combination termed A356, Bottom particulates of ash were heated to 400 degrees Celsius. Keep stirring the mixture for at least a few more minutes. In conclusion, continuous stirring resulted in a well-wetted state being achieved amid the matrix and the reinforcement. As may be seen in Figure 2 (a & b), the previously prepared hot metal is poured into a metal mould that has been heated beforehand. The casting process is iterated for diverse combinations of reinforcement along with matrix materials, including varying weight percentages of bottom ash particles with a

base alloy, that range from 0 to 8 weighted percent with weight percent increments of 2 weight percent). The Ready-Made Composite of Al A356 and Bottom Ash, as Depicted in Figure 3. The T6 heat-treatment procedure shows the first step of putting the material to a solutionizing temperature of 560°C for a span of 2 hours in a muffle furnace. This is followed by a rapid cooling process known as quenching, which is accomplished using oil. Subsequently, the material undergoes an artificial ageing process at a reading of 120 degrees Celsius maintained for a period of six hours.



Fig 1 : Electric Furnace



Fig 2: a) Pre Heating of Metal Mould b) Pouring of Molten Metal to Metal Mould



Fig 3: Prepared Al A356 - Bottom Ash Composite

2.3 Experimentation

The created composites of A356 reinforced with particles of Bottom Ash were put through a dry sliding wear test, and the results were compared to those of specimens in their as-cast and heat-treated states separately. The test samples had dimensions of 8 millimetres in diameter and 30 millimetres in length, and they were produced in accordance with ASTM standard G99-95 [16]. The pin on disc wear testing equipment that is standard is what is used to carry out the wear test. The outermost layer of the sample makes touch with a 62 HRC-hardened disc at some point throughout the testing process. The disc surface was composed of EN 32 steel, and it measured 165 millimetres in diameter, 8 millimetres in thickness, and had a surface hardness of roughly 0.84 micrometres. The disc's track diameter, as seen in Figure 5, was 120 mm. The recorded measurements were

taken at various intervals ranging from 5 to 45 minutes, with increments of 5 minutes. The magnitude of the frictional force, represented as F_N , was measured employing a force gauge with a precision of 1 Newton. Figure 4 depicts a schematic representation of pin-on-disc technology for your viewing pleasure. Various loads (which varied from 10 N through 40 N) and gliding rates (which varied from 1 m/s to 4 m/s) were used in the research on wear and friction. The loads ranged from 1 m/s to 4 m/s. The method of weight loss is utilised in the process of estimating the rate of wear. Right now, the data on the rubbing force are being used to conclude the coefficient of friction simultaneously with the force data. Data that has been acquired on the drysliding degradation research equipment can be found shown in Table 5.

The microstructure specimens underwent etching with Keller's reagent and were thereafter seen using SEM Micrography prior to undergoing microscopic examination with a standard metallographic approach. Figure 14 depicts the microstructure of samples that have been heat treated with varying amounts of their total weight. An SEM apparatus from the Czech Republic called TESCAN VEGA 3 LMU is used in the process of determining the form, appearance, and distribution of Bottom Ash particles that are found in combinations of A356 alloy. JDE 2300 is the programme that is utilised for the EDX research, and it is coupled with the SEM instrument. SEM analysis is performed on specimens For the purpose of microstructure investigation, the specimen under consideration has a diameter about 15 mm as well as a height measuring 5 mm. The surface of the specimen is first abraded utilising paper with grids with grit sizes of 240, 600, and 800. Subsequently, it is further refined by using polish paper having an overall thickness of 44 micro-metres. The object is subjected to a polishing process using a specialised machine and a velvet cloth, which facilitates the attainment of a refined and smooth surface finish. The specimens undergo a cleaning process using distilled water in order to eliminate any potential impurities, such as dirt as well as foreign particles, that could be present on the polished surface. Keller's reagent is ultimately responsible for etching the outermost layer of the specimen.

Studies using X-ray diffraction were carried out on A356 alloys composites in regulate to discover the various phases that are present in Al alloy matrices composites. The A356 alloy with 8 weight percent of Bottom Ash composite was chosen for the XRD experiments, and the specimen dimensions were 15 millimetres in diameter and 2 millimetres in height. Studies of XRD were performed with the assistance of PANA-LYTICAL XRD by using CU K radiation. The selection of the range of 2 was made with the intention of including all of the projected severe peaks associated with the material phases.

Table-5: Detailsofthepin-on-discmachinery

Discdiameter	120mm
Discspeed	0-1000 rpm
Normalload	0- 100 N
Leastcount	1 μ m
Power	230 V,AC50Hz
Discsurfacefinish	2 microns

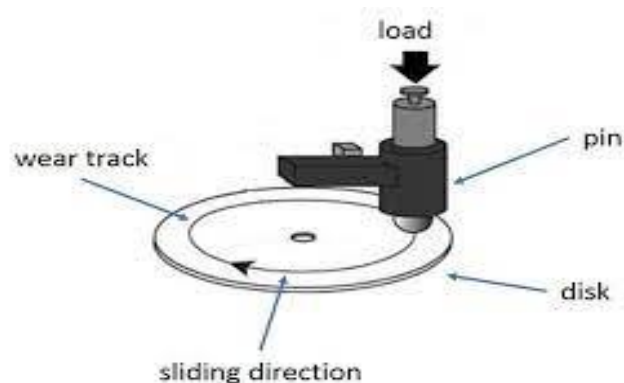


Fig. 4: Diagrammatic representation of pin-on disc equipment



Fig. 5: Pin-on-disc machinery

3. Result And Discussion

3.1 Effect of Applied load

The findings of a research investigating the impact of different weights on the rate of wear of composite specimens composed of A356-Bottom Ash in both their as-cast and treated with heat situation are shown in Figures 6 and 7, respectively. The experiments were conducted using altered loading conditions, spanning between 10 N to 40 N. The sliding velocity was maintained at 1 m/s, while the glide distance remained constant at 1500 metres. The findings indicate that the rate of degradation of as-cast composites exhibits a decline as the applied load increases up to the 8wt% threshold of reinforcement. However, beyond this threshold, no further alteration in the wear rate is seen. The aforementioned phenomenon was seen in the as-cast composites. When subjecting weights of 20, 30, as well as 40 newtons, a steady pattern is seen. The findings indicate that heat treatment leads to a comparable level of wear rate variation in the composite specimens. Additionally, the experimental results indicate that the composites subjected to heat treatment have a reduced overall wear rate when compared to the composites maintained in their original as-cast condition. It is evident from these findings that the composites that were heat treated had a greater resistance to wear, and it is advised that the composite that included 8wt% of reinforcements is stronger in comparison to the remaining composite materials owing to the evenly distributed distribution of Bottom Ash granules. [17,18].

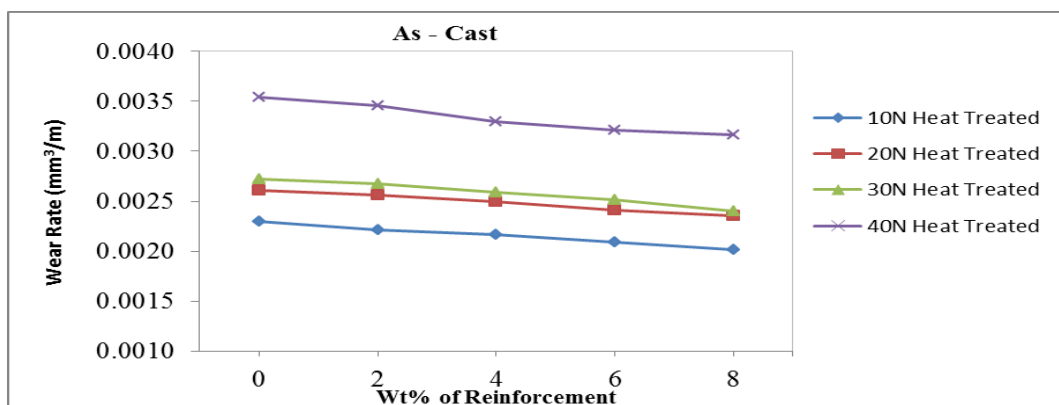


Fig 6: Comparison of wear rate with reinforcing % at various loads for as-cast Al A356 alloys and composites

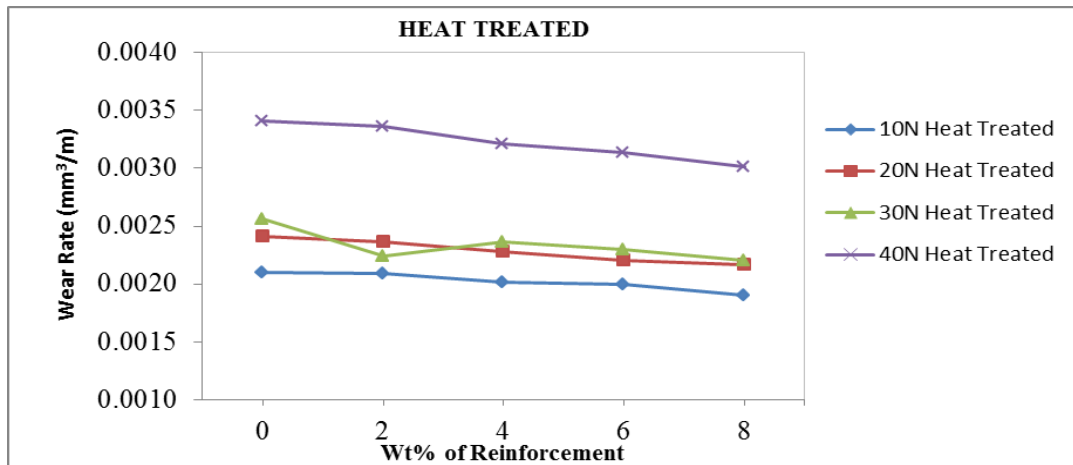


Fig 7: Wear rate variation with reinforcing % at various loads on heat-treated Al A3536 alloy with composites

3.2 EffectsofSlidingVelocity

The results of the change of wear rate at various sliding velocities on A356-Bottom Ash combinations of as-cast as well as heat treated specimens are shown in Figures 8 and 9, respectively. The sliding distance was held constant during all of the tests at 1500 metres, and the force was kept constant at 40 Newtons the whole time. This phenomenon was seen for the as-cast composites. The results showed the same trend whether the sliding velocity was 2 metres per second, 3 metres per second, or 4 metres per second. It has also been discovered that the rate of deterioration of the heat-treated composite is much lower when compared to the wear rate of the as-cast composite. The investigation revealed a positive correlation between the increase in speed and the corresponding rise in temperature. This temperature elevation facilitated the formation of a layer of oxide, subsequently resulting in a decrease in the rate of degradation of the composites. Because of the consistent distribution of Bottom Ash particles, it was discovered that the composite containing 8 weight percent of reinforcement is much more robust when when compared to the rest of the composites. The findings that were acquired in this study were comparable to the results that were obtained in previously published work accomplished by other researchers.

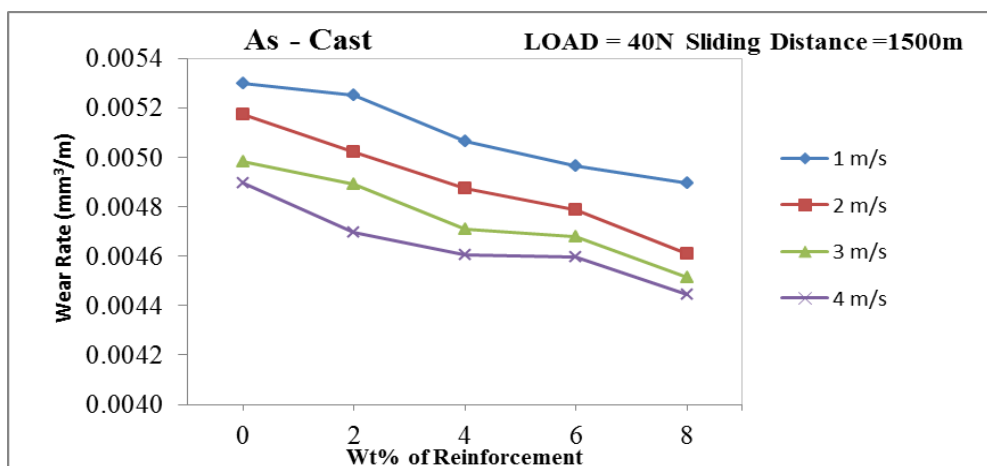


Fig 8: Wear rate variation at varied velocity of sliding for As-cast Al A356 alloys and composites

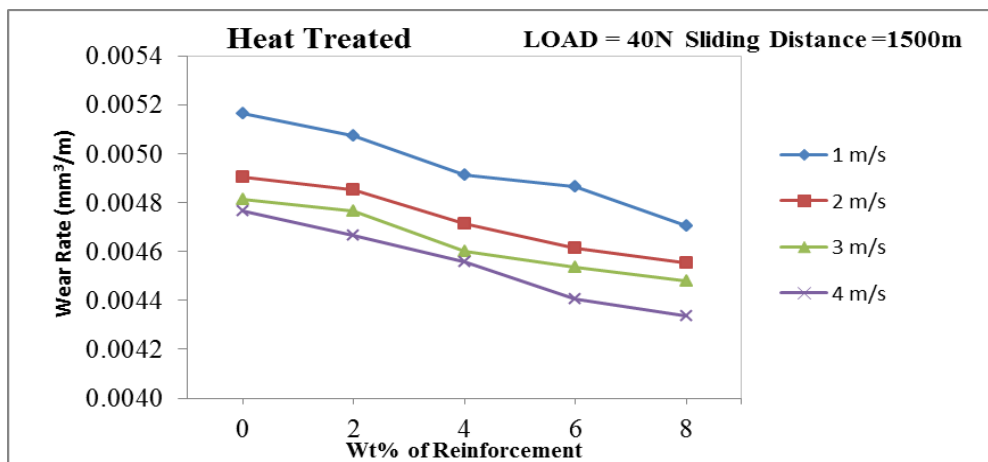


Fig 9: Wear rate variation at varying sliding velocity of heat-treated Al A356 alloys and composites

3.3 Friction Coefficient Effect (COF)

3.3.1 Effect of applied load

Figures 10 and 11 provide the outcomes of determining the friction coefficient for the A356 alloy and its composites in both the as-cast and heat-treated conditions. These calculations were conducted by considering different weight percentages of reinforcement and changing loading conditions. The tests were carried out with a fixed sliding velocity of one metre per second and a time interval of twenty-five minutes. Previous studies have shown that the amalgamation of stoneware particles into aluminium alloys in the form of a reinforcement shields the aluminium matrices from wear and reduces the severity of excessive surface shear strain. Because of this, the frictional force that is created among the disc and the specimen causes the coefficient of friction for composites to rise as the load is placed on them. This is in keeping with what was said before. Previous research carried out [19, 20] produced findings that were comparable to our results. It was also discovered that as the proportion of reinforcement grows, the co-efficient of friction decreases up to 8 weight percent of reinforcement. The decrease of COF composites is the explanation for the decline of COF in the composites. The composite parts of heat-treated specimens showed the same wear rate change regardless of load. Experimental results show that heat-treated composite samples have a lower coefficient of resistance than treatment composite specimens due to iron oxide and magnesium oxides. This is owing to composite composition [14,15].

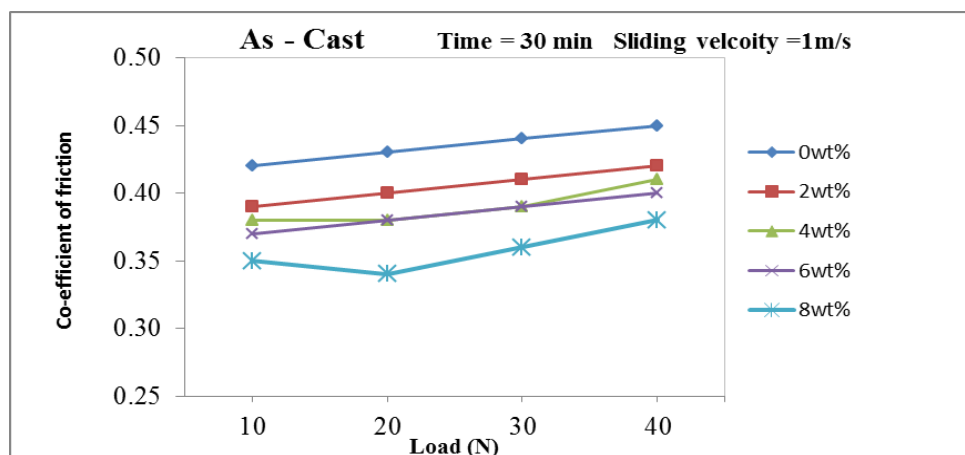


Figure. 10: Coefficient of resistance of Al A356 alloys and its mixtures under varied loads in as-cast state

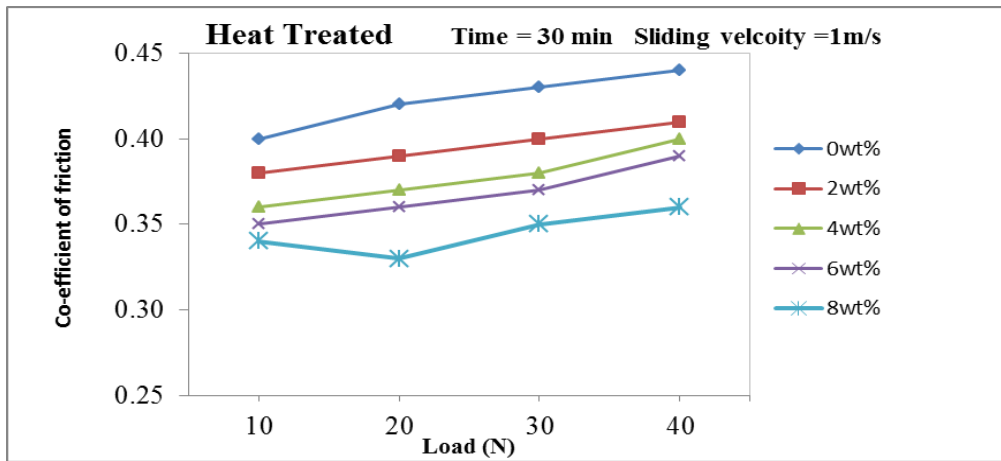


Fig 11: Coefficient of resistance of Al A356 alloys as well as its mixtures during heat treatment for varied loads

3.3.2 Sliding velocity effect

Figures 12, 13 show the results of the change of the rate of friction with the wt% of reinforcements at various sliding velocities for as-cast including heat treated specimens of A356 alloy as well as its composites. Up to 8 wt% of strengthening, it was shown that the index of friction decreased with increasing wear rate. Sliding faster causes the contact surface to heat up, creating an oxide layer that reduces wear. The same pattern was seen for the 2nd, 3rd, and 4th metres / second of sliding speed. Degradation rates for heat-treated composites were shown to fluctuate in a similar fashion. These results show that heat-treated composite specimens benefit from a reduced friction coefficient for the reason that of the incidence of iron oxide as well as magnesium oxide within the aggregates. [15-17].

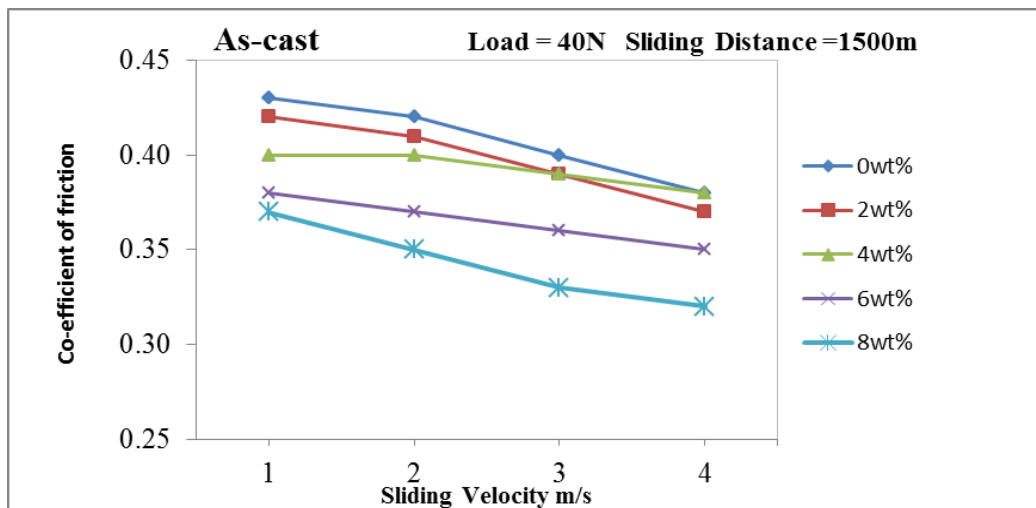


Fig 12: Al A356 alloy and composites' Coefficient of friction for varied velocity of sliding in as-cast state

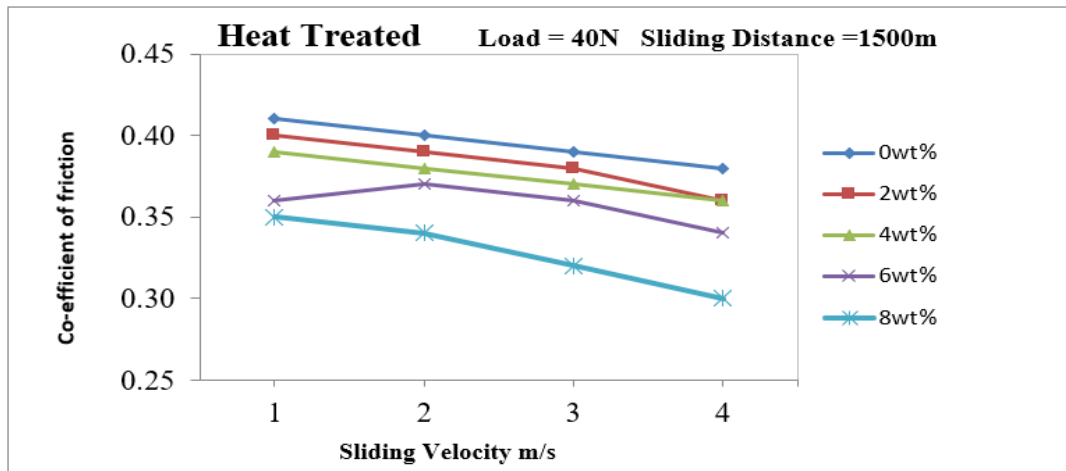
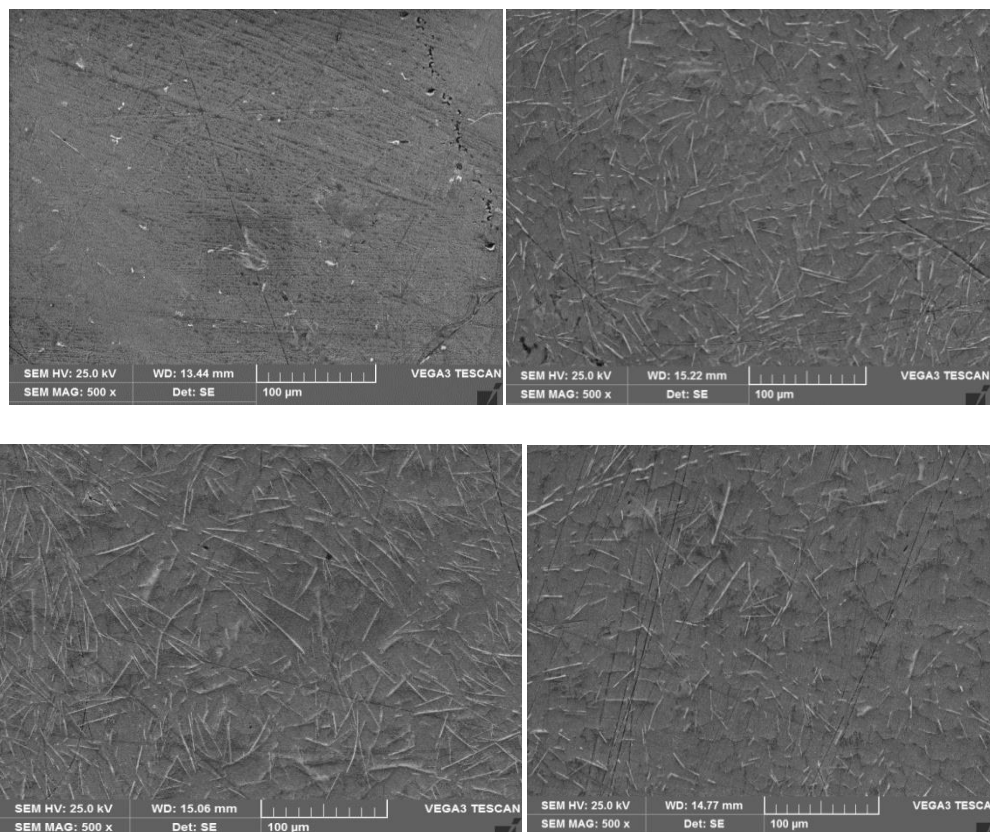


Fig 13: Variation of Al A356 alloy and composite friction coefficients at varied sliding speeds under heat-treated conditions

3.4 Micrographic Analysis

The morphology of the worms was examined using a microscope to have a better understanding of the different wear behaviours associated with the as-cast as well as its composite.



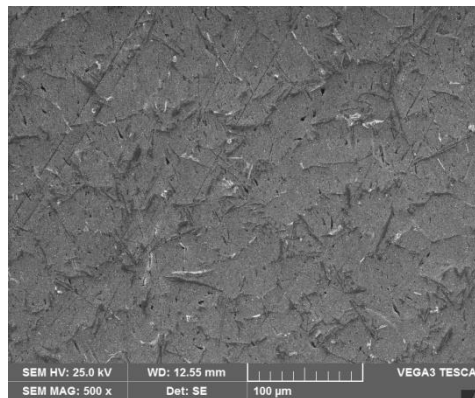


Fig. 14: SEM micrographs of samples of a) The alloy A356, b) 2.5% A356 of the composite c) A356/4 weight percent composite d) A356/6 weight percent composite, e) Composites with heat treatment at 500X magnification: A356-8Wt%.

According to the microscopy findings shown in Figure 14a-d, Bottom Ash particles were distributed equally over the A356 matrix at varying weight percentages. To continue attributing this success to the stirring, suitable process parameters must be used. The tribological characteristics of mixes may be enhanced by the homogeneous dispersion of Bottom Ash constituents and subsequent heat treatment. Al, Fe₂O₃, MgO, and Si may all be seen in the elemental examination of A356 containing 8wt% of Bottom Ash mixture shown in Figure 15. The presence of Fe₂O₃ and MgO in A356 alloy composites provides more evidence that Bottom Ash particles are present there. The X-ray diffractometer is used to analyse the Bottom Ash composites and the A356 alloy. In Figure 16a, we see the XRD pattern for the A356 alloy; the distinct aluminium phases can be seen at the different peaks. 390, 450, 650, and 780 at varied intensities. The Al phase peaks with an intensity of 390. The XRD pattern of A356 alloys containing 9 wt% of Bottom ash particles is seen in Figure 16.b. The different phases, such as Al and Fe₂O₃, are detailed. Fragments of Bottom ash phases can be recognised at 290, 470, 560, and 780, whereas the JCPDS patterns of the produced Al - Bottom ash compounds is 98-6077 at various 2 angles with varying intensities.

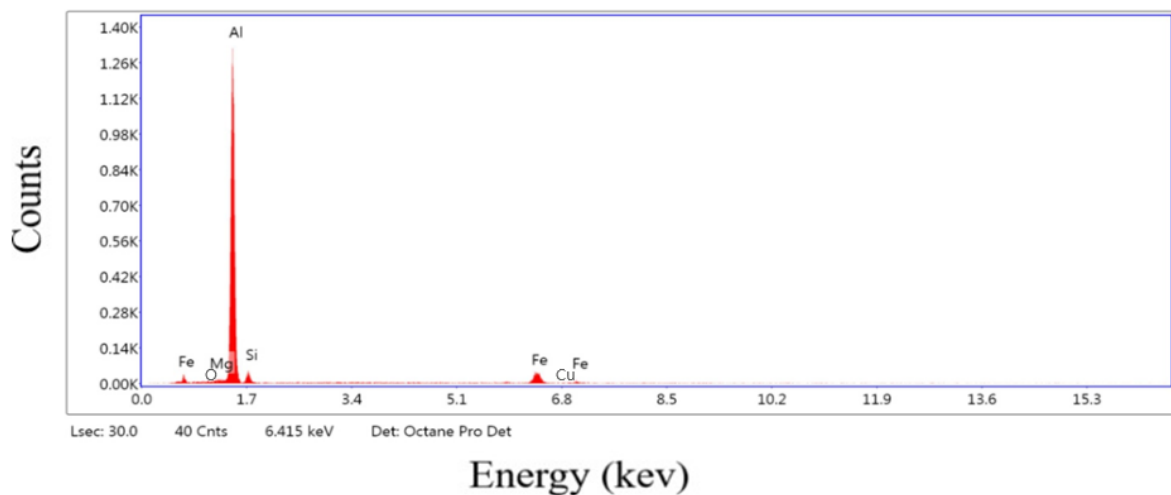


Fig 15: EDS spectrum of Al A356 with 8wt% of Bottom Ash particulate composite showing the presence of Fe₂O₃ particles

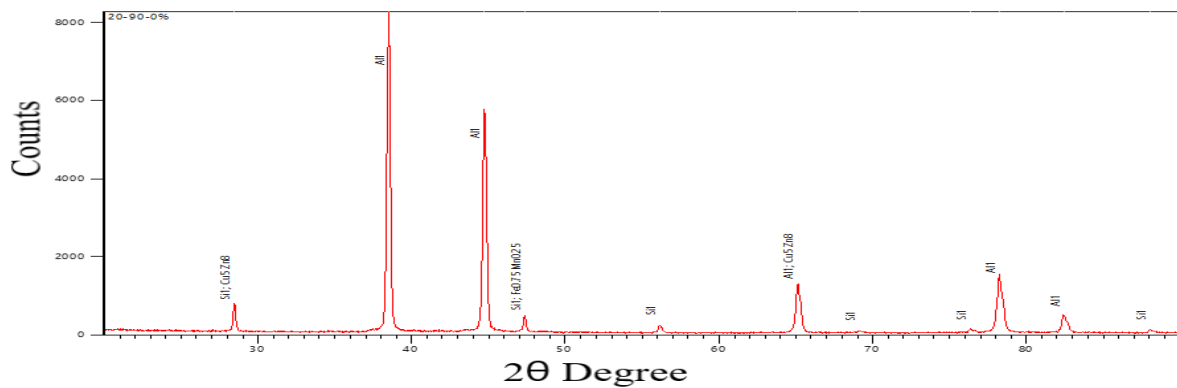


Fig. 16 (a) : X-raydiffractionofA356alloy

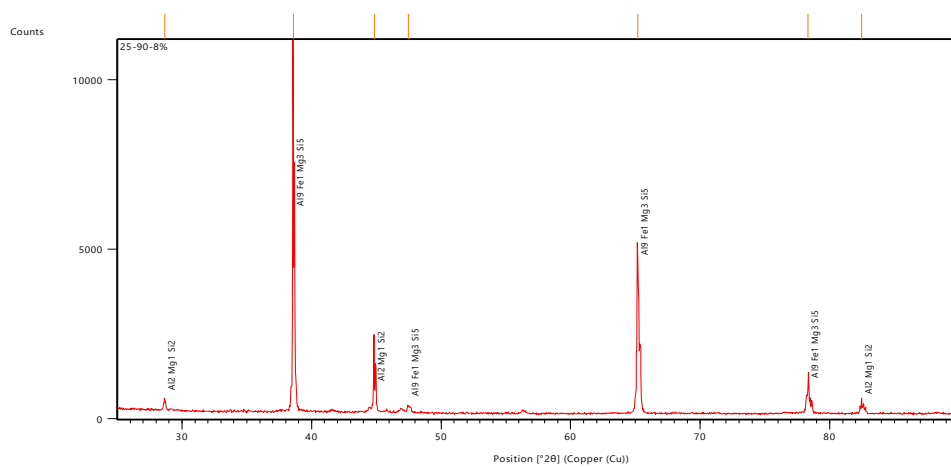


Figure 16 (b): .X-raydiffractionofA356-8wt% of Bottom ash

3.5 WornMorphology

The examination of the worn-out surfaces microstructure of A356 alloy, specifically A356/8wt% Bottom Ash particulate compositions, at 500X magnifications on both As-cast and heat-treated composite specimens is of utmost importance. Due to the comparatively smaller grain size of the A356 alloy matrix in relation to the roughened disc material, the viscous flow of the former becomes apparent during sliding, manifesting as a pin-shaped deformation on the surface of the specimen. Consequently, a significant quantity of material is wasted. On the worn surface of the A356 alloy, micropits and grooves, as well as a broken oxide layer, tribo layers, and separation, are seen in Figure 17 (a) and (b). Each of these features has the potential to contribute to an enhanced wear loss. Figure 17 (c) and (d) show that the incorporation of Bottom Ash to A356 alloys at a weight ratio of 8wt% increases the material's toughness by reducing the viscous motion of the matrix. This improvement can be observed in the material's durability and toughness. This is due to ferric oxide along with magnesium oxide being incorporated. The introduction of Bottom Ash particles resulted in a reduction in groove lengthening or abrasion, suggesting an increased vulnerability to wear loss [20]. Upon contrasting the as-cast as well as heat-treated combined specimens, it becomes evident that the brittleness and tribological attributes of the latter are substantially enhanced by heat treatment. Hard Rock Bottom Strain concentration seems to be occurring in and around ash pieces on A356 alloy, suggesting that these fragments are the primary transmission points of the stresses. The skin of a worm has fewer craters and pits. A smoother surface may be seen in micrographs obtained after 8wt% of material has been removed by heat treatment, as compared to the as-cast form.

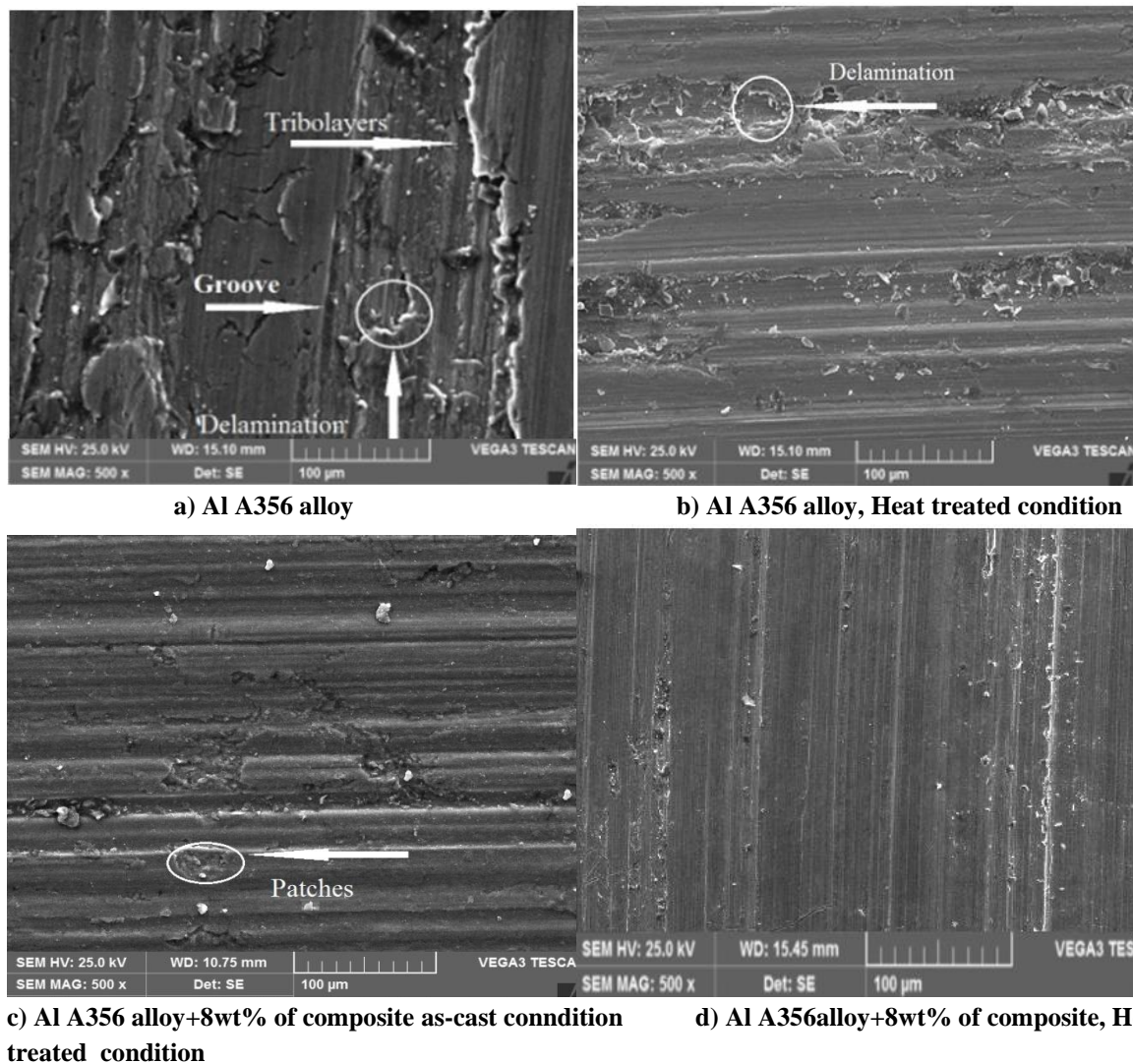


Fig 17: SEM images of the surface morphology of a) Al A356 alloy, b) Al A356 alloy Heat treated condition c) Al A356 alloy+8wt% of composite d) Al A356 alloy+8wt% of composite Heat treated condition at 500X magnification.

4. Conclusion

Bottom of the Al A356 Stir casting was the method that was used in the development of ash particle reinforced composites. The following inferences were drawn as a result The XRD study verifies the presence of Bottom ash particles stages in the Al A356 composite matrix, and the microstructural examination reveals that these particles are dispersed uniformly throughout the matrix.

- The microstructural study evidently shows that unvarying spreading of Bottom Ash
- Trial findings indicate that increasing sliding velocity and reinforcing weight percentage reduces wear rate. The wear rate rises with force.
- Sliding velocity and strengthening weight percent (wt%) lower coefficient of friction (COF). The COF also rises with load.
- Addition of Bottom Ash granules enhances cast A356 alloy wear resistance. A356 alloy and its mixes wear depending on load and sliding speed. Load as well as speed increased A356 alloy and Bottom Ash particle reinforced composite wear The testing indicated that increasing sliding velocity and reinforcing weight reduces wear. The wear rate rises with force.
- Sliding velocity and reinforcing percentage of weight (wt%) lower coefficient of friction (COF). The COF also rises with load.

References

- [1] American Society for Metals, ASM Handbook, Properties and selection. Nonferrous Alloys and Special-purpose Materials, ASM International hand book committee, Vol. 2, 1990, pp. 137-38.
- [2] MEIM. Schwartz, Composite material hand book, McGraw Hill, New York, 1984
- [3] Heinz A and Haszler A., Recent developments in aluminum alloys for aerospace applications, Material Science and Engineering, Vol. 1, 2000, pp. 102-107
- [4] M. V. Maisuradze, Yu. V. Yudin, and D. I. Lebedev, "Thermal strengthening of large parts made from high-strength sparingly doped steel in air," *Steel in Trans.*, 50(5), 61 – 66 (2020)
- [5] M. V. Maisuradze, M. V., Yudin, Y. V., Kuklina, A. A. et al. Effect of Heat Treatment on Mechanical Properties and Microstructure of Advanced High-Strength Steel. *Met Sci Heat Treat* 64, 522–527 (2023).
- [6] M. V. Maisuradze, M. A. Ryzhkov, and D. I. Lebedev, "Microstructure and mechanical properties of martensitic high-strength engineering steel," *Metallurgist*, 64(7 – 8), 640 – 651 (2020).
- [7] Shankar Subramanian, Balaji Arunachalam, Kawin Nallasivam, Alokesh Pramanik "Investigations on tribomechanical behavior of Al-Si10-Mg/sugarcane bagasse ash/SiC hybrid composites" Vol. 16, 2019, PP. 277-284.
- [8] S. Balakumar, Milon D. Selvam, and A. J. R. Nelson "Wear and Friction Characteristics of Aluminium Matrix Composites Reinforced With Flyash/Cu/Gr Particles" *International Journal of Chemtech Research*, Vol. 11, No. 01, 2018, PP 121-133.
- [9] Viney Kumara, Rahul Dev Gupta, N. K. Batra "Comparison of Mechanical Properties and effect of sliding velocity on wear properties of Al 6061, Mg 4%, Fly ash and Al 6061, Mg 4%, Graphite 4%, Fly ash Hybrid Metal matrix composite" *Procedia Materials Science* Vol 6, 2014, PP 1365– 1375
- [10] S. Mishra, A. Patnaik, S. R. Kumar "Comparative analysis of wear behavior of garnet and fly ash reinforced Al 7075 hybrid composite" *Materialwiss. Werkstofftech.* 2019, Vol 50, PP 86–96
- [11] Siva Prasad, A Rama Krishna, "Tribological Properties of A356.2/RHAC Composites" *Material Sci. Technol.*, vol 28, 2012, pp. 367-372. Elsevier Ltd.
- [12] P. Poza, M. A. Garrido, A. Rico, J. Rodriguez, "Dry sliding wear behavior of aluminium–lithium alloys reinforced with SiC particles", *Wear*, Vol. 262, 2007, pp. 292–300.
- [13] Prasad SV, McConnell BD. Tribology of aluminum metal-matrix composites: lubrication by graphite. *Wear*. 1991 Sep 30; 149(1-2): 241-53.
- [14] Ahmer SM, Jan LS, Siddig MA, Abdullah SF. Experimental results of the tribology of aluminum measured with a pin-on-disk tribometer: Testing configuration and additive effects. *Friction*. 2016 Jun; 4(2): 124-34.
- [15] Rohatgi PK, Tabandeh-Khorshid M, Omrani E, Lovell MR, Menezes PL. Tribology of metal matrix composites. In *Tribology for scientists and engineers 2013* (pp. 233-268). Springer, New York, NY.
- [16] Harti J, Prasad T B, Nagaral M, Jadhav P, Auradi V "Microstructure and dry sliding wear behaviour of AL2219-TiC composites" *Materials Today*, Vol 4, 2017, PP 11004-11009.
- [17] Madeva Nagaral, R. G. Deshpande. V. Auradi. Satish Babu Boppana. M. R. Anilkumar "Mechanical and wear characterization of ceramic boron carbide-reinforced Al 2024 alloy metal composites" *Journal of Bio and Tribo Corrosion*. 2021, PP 7-19 Springer.
- [18] Nagaral M, Auradi V, S. A. Kori, Hiremath V "Investigation on mechanical and wear behavior of nano Al₂O₃ particulates reinforced AA7475 alloy composites" *Journal of Mechanical Engineering Science*. Vol 13, 2019, PP 4623-4635.
- [19] Wang W, Du A, Fan Y, Zhao X, Wang X, Ma R Q "Microstructure and tribological properties of SiC matrix composites infiltrated with an aluminium alloy" *Tribol Int*, Vol 120, 2018, PP 369-375
- [20] V. C. Uvaraja, Natarajan Nanjappan, K. Shivkumar. S. Jagadeshwaran "Tribological behaviour of heat reacted Al 7075 aluminium metal matrix composites" *Indian journal of engineering and materials science* vol 22, 2015, PP 51-61.
- [21] Pramanik A. Effects of reinforcement on wear resistance of aluminum matrix composites. *Transactions of Nonferrous Metals Society of China*, Vol 26, 2016, pp. 348-358.

- [22] Tribological study on effect of chill casting on aluminium A356 reinforced with Bottom ash/paticulated composites, Sunil Kumar M, Sathisha N, Jaganatha N, Batluri Tilak Chandra, Journal of Bio and Tribo Corrosion (Q1), Vol 8, Issue 52, 2022, Springer.
- [23] Aigbodion V, Atuanya C, Edokpia R, et al. Experimental study on the wear behaviour of Al-Cu-Mg/bean pod ash nano-particles composites. Transactions of the Indian Institute of Metals, Vol 69(4), 2016, PP971-977
- [24] Harti J, Prasad T B, Nagaral M, Jadhav P, Auradi V. Microstructural and dry sliding wear behaviour of Al2219-TiC composites; Materials Today: Proceedings 4(2017), PP11004–11009
- [25] Q.D. Qin, Y.G. Zhao, W. Zhou, “Dry sliding wear behavior of Mg₂Si/Al composites against automobile friction material”, Wear, Vol. 264, No. 7-8, 2008, pp. 654-661.
- [26] Tribo mechanical study on aluminium A356 reinforced metal matrix composites casted with copper chill, Sunil Kumar M, Sathisha N, Jaganatha N, Journal of Bio and Tribo Corrosion (Q1), Vol 9, Issue 56, 2023, Springer.
- [27] H.S. Sridhar, S. Sanman b, T.B. Prasad, Batluri Tilak Chandra, “Effect of reinforcement and applied load on three-body dry sand abrasive wear behavior of A356 bottom ash metal matrix composites” ScienceDirect, ELSEVIER Mater.Today: Proc. 26 (2020) 2814–2816. <https://WWW.sciencedirect.com/science/article/abs/pii/S2214785320313419>.
- [28] Siva Prasad A Rama Krishna, “Tribological Properties of A356.2/RHA Composites” Material Sci. Technol, Vol 28, PP 367-372. Elsevier Ltd.